

# Fabrication of $Zn_4Sb_3$ Bulk Thermoelectric Materials Reinforced with SiC Nanosized Particles by Hot Extrusion Process

Takahiro Akao, Kenji Uya, Tetsuhiko Onda, and Zhong-Chun Chen

**Abstract**— Zinc antimonide,  $Zn_4Sb_3$ , has been found as a promising thermoelectric material utilized in a temperature range of 200 ~ 500°C, in which there exist vast waste-heat resources exhausted from many factories and vehicles. However, the compound intrinsically shows an extremely brittle feature being an impediment for practical applications. Thus, enhancement of the mechanical properties is highly crucial to prevent unexpected fractures during manufacturing and service processes of modules. We have focused on incorporating nanosized SiC particles into  $Zn_4Sb_3$  matrix. The bulk samples were prepared by mechanochemical mixing of the starting powders and subsequent hot-extrusion process. The extrudates containing SiC particles up to 5vol% exhibited sound appearances, high density, and fine-grained microstructures with single phase of  $Zn_4Sb_3$ . The mechanical properties such as hardness and compressive strength are remarkably improved by the addition of SiC particles, as a result of dispersion strengthening of SiC particles and microstructural refinement induced by a pinning effect of the particles. Meanwhile, the thermoelectric properties are retained comparable to the pristine compound, in contrast to a conventional behavior where the reinforcements in a semiconductor should usually role-play as an impurity.

**Keywords**—hot extrusion, thermoelectric materials, reinforcement, SiC particles

## I. INTRODUCTION

IN recent years, global warming has become one of the most serious issues due to excessive consumption of fossil fuels. Furthermore, it can be predicted that fossil fuel resources must be exhausted in the not-too-distant future if they continue to be consumed without restraint. So the energy-saving technologies have been intensively developed over the past decade. As one of the technologies, thermoelectric generation has drawn much attention for being a clue to solve the problem, since vast amount of waste heat, exhausted from a number of industrial plants, vehicles, home heating and so on, is still unused [1]. The thermoelectric generators which consist of a module with both p- and n-type semiconducting thermoelectric materials, can convert heat to electricity directly based on the Seebeck

effect. On the other hand, the module can also create heat flux through consumption of electrical energy, mainly used for cooling, based on the Peltier effect. For evaluation of the efficiency of thermoelectric materials, the dimensionless figure of merit ( $ZT$ ), calculated by following equation, is conventionally taken into account.

$$ZT = \frac{\alpha^2 T}{\rho \kappa} \quad (1)$$

Where  $\alpha$  is the Seebeck coefficient or thermopower,  $\rho$  the electrical resistivity,  $\kappa$  the thermal conductivity and  $T$  the absolute temperature. From the above equation, a good thermoelectric material should have higher thermopower and lower thermal conductivity.

The compound of zinc and antimony,  $Zn_4Sb_3$ , was found as a p-type thermoelectric material with an excellent performance in a temperature range of 200 ~ 500 °C, for example,  $ZT = 1.3$  at 400°C [2]. Moreover,  $Zn_4Sb_3$  can be a suitable candidate of the thermoelectric generator for above-mentioned waste-heat resources not only because of its high efficiency, but because of relatively low toxicity compared to other lead-containing thermoelectric materials. However, this compound intrinsically shows an extremely brittle feature being an impediment for practical applications. Thus, enhancement of the mechanical properties is indispensable key to utilize the material practically, hence avoiding unexpected fractures during manufacturing and service processes of modules. To enhance fracture strength and toughness, reinforcements such as fibers or particles have been extensively used, so far. In particular, for a brittle functional material, nanosized particles are used in order to avoid an introduction of sources of fracture and/or degradation brought by the inclusions. So, we have focused on incorporating nanosized SiC particles into  $Zn_4Sb_3$  matrix.

Extrusion is one of practical techniques for industrial applications because of its merits of continuously manufacturing elongate products with various cross-section shapes. Moreover, a fine-grained microstructure and preferentially oriented texture may be achieved, which arise from large shear strain subjected and dynamic recrystallization driven during hot-extrusion process [3].

In this paper, we investigate the effect of addition of

T. Akao, Department of Mechanical and Aerospace Engineering, Tottori University (phone: +81-857-31-6760; fax: +81-857-31-5210; e-mail: akao@mech.tottori-u.ac.jp).

K. Uya, T. Onda, and Z.-C. Chen, Department of Mechanical and Aerospace Engineering, Tottori University (e-mail: chen@mech.tottori-u.ac.jp).

nanosized SiC particles on the extrusion behavior, mechanical and thermoelectric properties of hot-extruded  $Zn_4Sb_3$  bulk materials.

## II. EXPERIMENTAL

Starting powders of pure metallic zinc and antimony (Kojundo Chemical Lab., >99.7% purity) and nanosized silicon carbide particles (Wako Chemical, 50 nm in average) were all weighted to be nominal compositions of  $Zn_4Sb_3 - x$  vol% SiC ( $x$  ranges from 0 to 5), and roughly mixed in a mortar. Then the mixture was subjected to mechanically-activated milling in ethanol medium in a planetary ball milling system for 4 hours, in order to refine the sizes of the powders, mix them homogeneously, and promote the reactions between the powders during subsequent hot-extrusion process. Subsequently, the powder mixture was formed into a cylindrical green compact (20 mm in diameter and 20 mm in length) by uniaxial press, and vacuum-encapsulated into an aluminum can to obtain an extrusion billet. The hot extrusion was performed at 450°C with an extrusion ratio of  $R = 7$  and punch speed of 1 mm/min. It is noteworthy that, prior to the extrusion operations, the billet was heated and kept for 20 min., thereby the reaction between zinc and antimony occurs to form  $Zn_4Sb_3$  compound.

Density of the extruded samples was determined by the Archimedes method. X-ray diffraction (XRD) using  $Cu-K\alpha$  radiation and field emission scanning electron microscopy (FE-SEM) were performed to characterize the phase and microstructure, respectively. The mechanical properties at room temperature were evaluated using the following methods, hardness by the Vickers hardness tests at a load of 9.8 N, fracture toughness by the indentation tests, and compressive strength by the uniaxial compression tests with cylindrical samples.

The Seebeck coefficient and electrical resistivity of the samples were simultaneously measured using a thermoelectric property test apparatus (ULVAC-RIKO Ltd., ZEM-3). The thermal conductivity of the samples was calculated from the measured values of density, heat capacity and thermal diffusivity. The heat capacity and thermal diffusivity were measured using a laser flash measurement apparatus (ULVAC-RIKO Ltd., TC-7000). The dimensionless figure of merit of the samples was calculated by (1).

## III. RESULTS AND DISCUSSION

As for the hot-extrusion process for samples with different contents of SiC particles, the extrusion pressure vs. stroke curves are shown in Fig.1. All the curves seem to be similar to each other. From the start point A to B, the  $Zn_4Sb_3$  powder

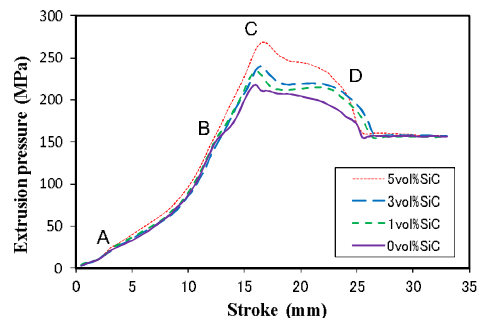


Fig. 1 Extrusion pressure vs. stroke curves under the conditions of  $R = 7$  at 450°C.

inside the Al can is further compacted. At the same time, the plastic deformation of Al sheath occurs. At point B, the Al alloy in the front end of the billet starts to be extruded out of the die. At point C, where the pressure reaches to maximum,  $Zn_4Sb_3$  rod, surrounded by the sheath, starts to be formed. Subsequently, the extrusion pressure is gradually reduced and the extrusion of the compound steadily continues up to point D. Finally the compound inside the billet is completely consumed, and only residual aluminum sheath is extruded. As a result, the pressure rapidly settles down to nearly the same value. The maximum pressure tends to increase with increasing the SiC particle content, reflecting an enhancement of deformation resistance of the billet with the addition of SiC particles in  $Zn_4Sb_3$  matrix.

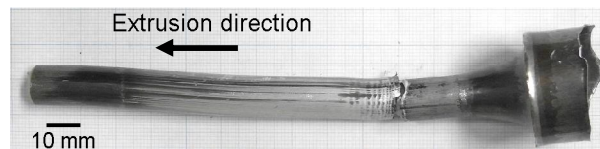


Fig. 2 A typical example of the appearance of an extruded sample.

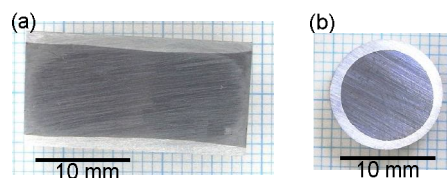


Fig. 3 Typical pictures of (a) longitudinal-section and (b) cross-section of an extruded sample.

Fig.2 shows a typical example of the appearance of a hot-extruded product. It seems that there are no evident defects in the extrudate and the hot extrusion successfully proceeds throughout the process. And from the sectional views shown in Fig.3, there is a good joining between the  $Zn_4Sb_3$  compound and aluminum sheath, which show dark gray and bright contrasts, respectively. It is found that a dense and crack-free bulk extrudate can be obtained under the conditions used in the present work.

The relative density of the extruded samples and the green compacts with different contents of SiC particles is shown in Fig.4. The density of green compacts looks like insensitive to SiC content, whereas the density of extruded samples shows a slight decrease with increasing SiC content. The reduction

tendency of density is apparently attributed to the inhibitory effect of SiC particles on densification of  $Zn_4Sb_3$  matrix.

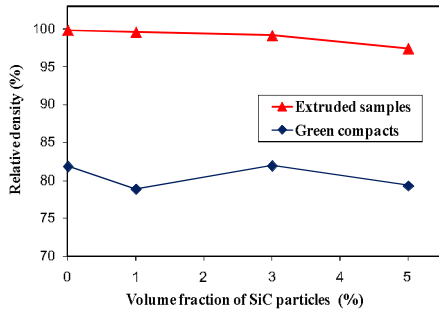


Fig. 4 Relative density as a function of volume fraction of SiC particles for compacted and extruded samples.

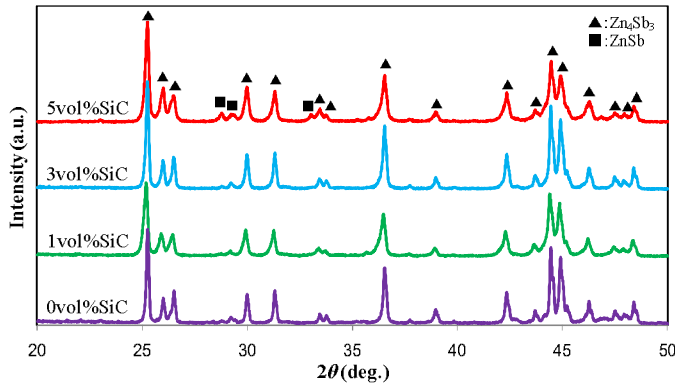


Fig. 5 XRD patterns of hot-extruded  $Zn_4Sb_3$  samples with addition of SiC particles.

Nevertheless, its degree is not so significant and the density exhibits high values of more than 98% even for the sample with 5 vol%SiC addition.

Fig.5 shows the XRD patterns of the extruded samples with different contents of SiC particles. From the patterns, except for faint traces of ZnSb observed in 5 vol%SiC sample, all other peaks are attributed to the  $Zn_4Sb_3$  phase. It is confirmed that these samples consist of almost  $Zn_4Sb_3$  single phase. There is no trace of the SiC phase found in all the patterns, mainly because of fine grain sizes and small amount of the SiC particles. In addition, relatively broaden peaks are observed in 1 vol%SiC sample, implying that the crystallite size could be reduced as compared with the other samples.

The SEM images of fracture surfaces of the extruded samples with different SiC contents are shown in Fig.6. These fractographs indicate that, with increasing the SiC content, the grain size of the matrix is reduced and also surface relief becomes small and complex. This can be explained by grain refinement caused by a pinning effect of SiC nanosized particles during dynamical recrystallization of the extrusion process and/or crack deflection induced by SiC particles. Furthermore, on those fracture surfaces with higher SiC contents, some regions with submicron sizes and dark contrast can be observed,

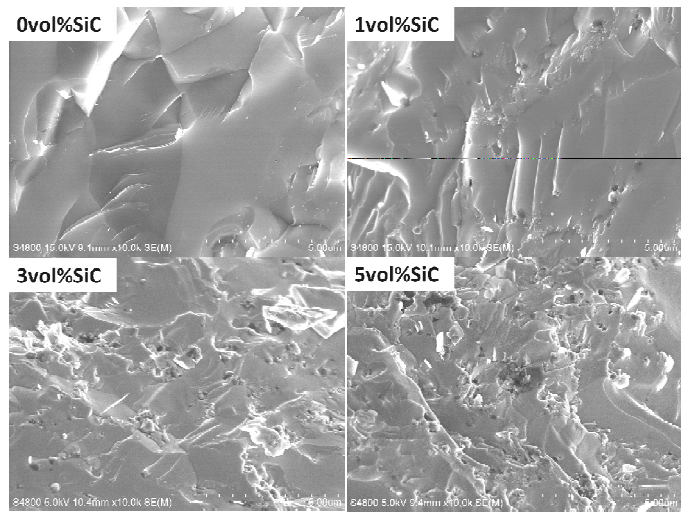


Fig. 6 SEM images of the fracture surfaces of extruded  $Zn_4Sb_3$  samples with addition of SiC particles.

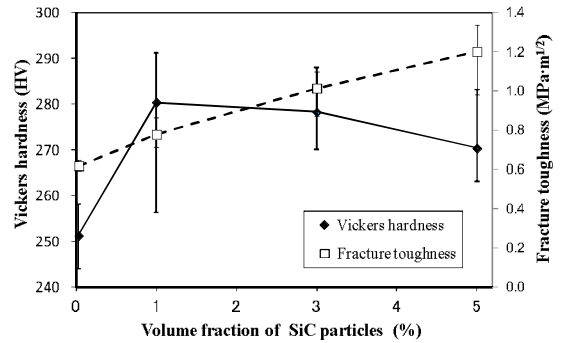


Fig. 7 Vickers hardness and fracture toughness of extruded  $Zn_4Sb_3$  samples as a function of volume fraction of SiC particles.

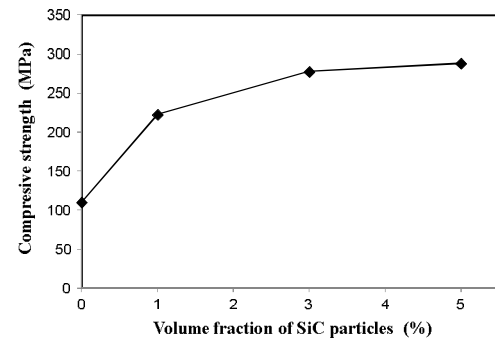


Fig.8 Compressive strength of extruded  $Zn_4Sb_3$  samples as a function of volume fraction of SiC particles.

presumably resulting from the agglomeration of nanosized SiC particles.

Vickers hardness and fracture toughness of the extruded samples as a function of volume fraction of SiC particles are illustrated in Fig.7. Both hardness and fracture toughness increase with addition of the SiC particles compared with pure  $Zn_4Sb_3$  sample (0%SiC). The fracture toughness is monotonically enhanced with the increase in volume fraction of SiC particles up to 5 vol%, while the hardness reaches a peak at a relatively low SiC content of 1 vol%. This behavior of hardness change can be explained by the density reduction and

agglomeration of SiC particles as mentioned above. On the other hand, the fracture toughness is enhanced with increasing SiC content, even though the agglomeration of SiC particles occurs. This result suggests that there may exist an optimal SiC particle size, which seems larger than a scale of tens of nanometers used in the current work, from the viewpoint of toughness improvement of  $Zn_4Sb_3$  matrix. Thus the agglomerated SiC particles are expected to work as a reinforcement more effectively than isolated nanosized particles. Fig.8 shows the compressive strength of the extruded  $Zn_4Sb_3$  samples as a function of volume fraction of SiC particles. The compressive strength increases with increasing the SiC particles, and reaches a value of almost three times of that of pure  $Zn_4Sb_3$  sample. This tendency agrees well with the fracture toughness. The above results have demonstrated that the incorporation of SiC nanosized particles does result in microstructural refinement and strengthening/toughening of  $Zn_4Sb_3$  matrix.

The temperature dependence of electrical resistivity and the

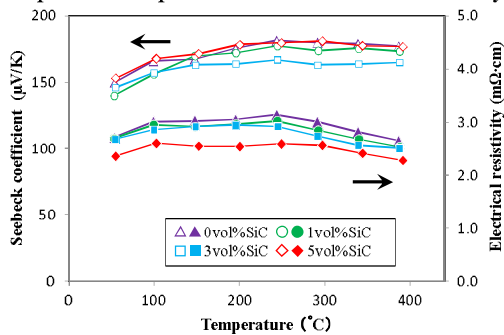


Fig. 9 Temperature dependence of the Seebeck coefficient and electrical resistivity of extruded  $Zn_4Sb_3$  samples. The filled and unfilled symbols indicate electrical resistivity and the Seebeck coefficient, respectively.

Seebeck coefficient of the extruded  $Zn_4Sb_3$  samples with different SiC contents was measured as shown in Fig.9. The Seebeck coefficient in the measured temperature range appears less sensitive to the SiC content owing to small amounts of the SiC particles in the present study. The resistivity, however, apparently decreases with increasing the SiC content. This behavior seems to be an exception to the traditional electron scattering theory, in which the dispersion of nonconductive particles in a matrix results in an increase in electrical resistivity due to reduction of electron mobility by interfacial scattering. This kind of behavior has also been confirmed in other cases of SiC reinforced p-type thermoelectric materials [3], [4]. Accordingly, it is possible that the SiC particles act as conductive inclusions with a high carrier density induced by doping of metallic constituents of matrix.

Fig.10 shows the temperature dependence of thermal conductivity of the extruded  $Zn_4Sb_3$  samples with different SiC contents. The thermal conductivity significantly decreases when 1 vol% SiC particles were added, but further addition of SiC particles leads to a considerable increase in thermal

conductivity. Since the thermal conductivity of SiC is known to be as high as  $\sim 100$  W/mK, the addition of SiC basically increases the bulk thermal conductivity. In the case of the sample with 1 vol% SiC particles, the grain size of the matrix is largely refined as suggested by the XRD pattern, resulting in low thermal conductivity due to an enhancement of phonon scattering at grain boundaries [5].

Finally, the temperature dependence of dimensionless figure of merit calculated by (1) using the parameters mentioned above

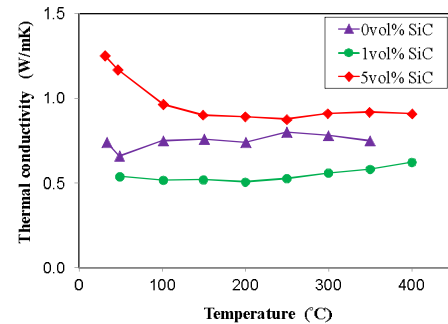


Fig. 10 Temperature dependence of thermal conductivity of extruded  $Zn_4Sb_3$  samples.

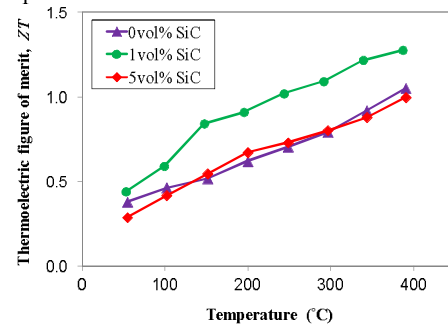


Fig. 11 Temperature dependence of dimensionless thermoelectric figure of merit of extruded  $Zn_4Sb_3$  samples.

is drawn in Fig.11. As a result, the sample with 1 vol% SiC particles shows the maximum  $ZT$  of 1.28 at  $400^\circ\text{C}$  in the present study, the value is comparable to the value reported for a hot-pressed sample [2]. It is noteworthy that even for the sample with 5 vol% SiC particles, the  $ZT$  value retains almost the same as that of the pure  $Zn_4Sb_3$  sample, while the compressive strength is three times higher as stated above. Consequently, the SiC nanosized particles behave to be of significance for strengthening the  $Zn_4Sb_3$  bulk materials prepared by the hot-extrusion technique.

#### IV. CONCLUSIONS

The SiC nanosized particles reinforced  $Zn_4Sb_3$  bulk materials have been successfully prepared by a hot-extrusion technique. The extruded samples exhibit good mechanical properties and moderate thermoelectric properties. The sample with 5 vol% SiC particles shows compressive strength three times higher than pure  $Zn_4Sb_3$  sample, while it remains comparative thermoelectric properties. In the case of the sample with 1 vol% SiC, it has the maximum  $ZT$  of 1.28 at

400°C. Therefore, it is concluded that the SiC reinforcement can provide a significant improvement for strengthening the  $Zn_4Sb_3$  prepared by the hot-extrusion technique.

#### ACKNOWLEDGEMENTS

The authors thank Prof. Takashi Ito in EcoTopia Science Institute, Nagoya University, for experimental support and fruitful discussions. This work was supported in part from JFE 21st Century Foundation and from EcoTopia Science Institute at Nagoya University.

#### REFERENCES

- [1] G. J. Snyder, and E. S. Toberer, "Complex thermoelectric materials", *Nature Materials*, vol. 7, pp.105-114, Feb. 2008.
- [2] T. Caillat, J.-P. Fleurial, and A. Borshchevsky, "Preparation and thermoelectric properties of semiconducting  $Zn_4Sb_3$ ", *J. Phys. Chem. Solids*, vol. 58(7), pp.1119-1125, 1997.
- [3] Z. Chen, J. Tsujimura, and F. Fujita, "Processing and thermoelectric properties of  $Zn_4Sb_3$  compound by powder extrusion technique", *Powder Metall. & Particulate Mater.*, pp.229-237, 2008.
- [4] D. W. Liu, J.-F. Li, C. Chen, and B.-P. Zhang, "Effects of SiC nanodispersion on the thermoelectric properties of p-type and n-type  $Bi_2Te_3$ -based alloys", *J. Electron. Mater.*, vol. 40(5), pp.992-998, 2011.
- [5] J. W. Sharp, S. J. Poon, and H. J. Goldsmid, "Boundary scattering and the thermoelectric figure of merit", *Phys. Stat. Sol. (a)*, vol. 187(2), pp.507-516, 2001.